Geomechanics and Engineering, *Vol. 39, No. 3 (2024) 241-256*
https://doi.org/10.12989/gae.2024.39.3.241

The effect of soil physical properties on predicting shear strength parameters based on comparing ensemble learning, deep learning, and support vector machine models

Ba-Quang-Vinh Nguyen*[1,2] and Yun-Tae Kim[3a]

[1]*School of Civil Engineering and Management, International University, Ho Chi Minh City, Vietnam*
[2]*Vietnam National University, Ho Chi Minh city, Vietnam*
[3]*Ocean Engineering Department, Pukyong National University, Busan, Korea*

(*Received November 3, 2023, Revised October 5, 2024, Accepted October 14, 2024*)

Abstract. The shear strength (SS) of soil is a critical parameter utilized in the design of civil engineering projects. The SS parameters, including cohesion (c) and friction angle (φ), can be determined through methods conducted either in the field or within a laboratory environment. However, the traditional method for determining SS parameters are not only costly but also time-consuming. Recently, the application of machine learning (ML) in geotechnical problems has received increasing attention. In order to select an appropriate ML model and assess the effect of physical properties on the SS of soil. This research endeavors to predict critical SS parameters of soil through the application of five machine learning (ML) models, integrating easily-available physical soil index, including specific gravity (G), saturation degree (Sr), liquid limit (LL), silt content (SC), and clay content (CC). The used ML techniques include Extreme Gradient Boosting (XGBoost), Random Forest (RF), Multilayer Perceptron (MLP), Support Vector Machine (SVM), and Convolutional Neural Network (CNN). A range of metrics, encompassing the root mean square error (RMSE), mean absolute error (MAE), and determination coefficient (R^2) were used to measure the predictive efficacy of the employed models as well as compare the performance of the used ML models. The values of R^2 range from 0.769 to 0.987 indicate that all ML models exhibit excellent predictive capabilities for estimating SS parameters, in which the XGBoost, and CNN techniques show outperforming results compared to the other models. The study uses decision tree feature importance (DTFI) and coefficient feature importance (CFI) techniques to investigate how various physical properties impact the predictive capabilities of the model and indicates that both G and LL have a substantial impact on the predictive accuracy of cohesion and friction angle.

Keywords: cohesion; deep learning; ensemble learning; feature importance; friction angle; support vector machine

1. Introduction

Shear strength (SS) of soil is the internal resistance that a mass of soil can provide to withstand failure and sliding along any plane within it (Yoseph 2022). The stability of excavations, earth dams, hillside slopes, the foundations of structures, and various other geotechnical engineering concerns rely on the SS of soil (Murthy 2002). Therefore, SS is a crucial parameter employed to evaluate the mechanical behavior of soil and plays a pivotal role in designing and constructing geotechnical structures (Chitra and Gupta 2014).

Following the principles of the Mohr-Coulomb Failure Criterion, shear strength is influenced by two fundamental factors: cohesion (c), and friction angle (φ). Which, c can be described as the resistance of displacement of soil particles, arising from a combination of bonding strength among soil particles, and the surface tension of retained water (Mollahasani *et al.* 2011), while φ defines the maximum angle between a horizontal plane and an inclined plane where soil particles remain in equilibrium (Yoseph 2022).

The SS parameters can be determined through techniques conducted either in the field or in a laboratory setting. Common laboratory tests include the Direct Shear Test and the Triaxial Compression Test. In-situ tests comprise methods like the Standard Penetration Test (SPT), Cone Penetration Test (CPT), Pressuremeter Test, and Vane Shear Test. Nonetheless, the procedure for measuring SS parameters, whether in the field or a laboratory, inherently entails high costs, consumes significant time, and demands substantial labor input (Khanlari *et al.* 2012, Mohammadi *et al.* 2022, Zakharov *et al.* 2022). Moreover, securing accurately undisturbed soil samples from the field presents substantial challenges. This is due to various factors, including the handling and transportation of samples, the release of overburden pressure, and the maintenance of optimal laboratory conditions. Consequently, careful oversight and attention are imperative throughout the entire process (Yoseph 2022).

The initial soil data to be determined in any geological survey typically revolves around the soil's physical characteristics. It's a well-established fact that the soil's physical properties enable the estimation of the SS parameters. The soil's composition, texture, particle size,

*Corresponding author, Ph.D.
E-mail: nbqvinh@hcmiu.edu.vn
[a]Professor

ISSN: 2005-307X (Print), 2092-6219 (Online)

clay minerals type, and water content all contribute to soil cohesion (Hosseini *et al.* 2018, Zakharov *et al.* 2022). In addition, particle size distribution, particle shape, water content, void ratio, fine content, liquid limit, and density all influence the friction angle (Jain *et al.* 2010, Mousavi *et al.* 2011). Therefore, some researchers have proposed a range of models for estimating the SS parameters by taking into account various physical properties, such as soil type, grain size distribution, density, water content, Atterberg limits, void ratio, saturation, etc... Numerous empirical equations have been developed for the estimation of the SS parameters through both regression and multiple regression methods (Adunoye 2014a, b, Ersoy *et al.* 2013, Roy *et al.* 2019, Goktepe *et al.* 2008). These formulas were presented as follows.

$$c = 265\left(\frac{PI}{LL}\right)^{2.78} \quad (1)$$

$$c = -0.525 + 0.241G \quad (2)$$

$$c = 0.685FC \quad (3)$$

$$c = 5.287e^{0.028FC} \quad (4)$$

$$c = 27.21\ln(FC) - 65.28 \quad (5)$$

$$c = -0.004FC^2 + 1.118FC - 7.383 \quad (6)$$

$$\varphi = -204.5\left(\frac{PI}{LL}\right)^2 + 53.6\frac{PI}{LL} + 31 \quad (7)$$

$$\varphi = -29.604 + 34.22\rho \quad (8)$$

$$\varphi = -0.404FC + 38.06 \quad (9)$$

$$\varphi = -16.3\ln(FC) + 78.07 \quad (10)$$

$$\varphi = -0.001FC^2 - 0.571FC + 41.4 \quad (11)$$

* (1): Ersoy *et al.* (2013); (2): Roy and Dass (2014); (3), (4), (5), (6): Adunoye (2014b); (7): Ersoy *et al.* (2013); (8): Roy and Dass (2014); (9), (10), (11): Adunoye (2014a)

where, PI is a plastic index (%), LL is a liquid limit (%), FC is a fine content (%), G is a specific gravity, ρ is a density (g/cm^3).

In research conducted by Ersoy *et al*. (2013), empirical Eqs. (1) and (7) using multiple regression analysis revealed correlations between friction angle, cohesion and plasticity properties of clayey soil. The findings of this study propose that cohesion and friction angle can be estimated from plastic limit and liquid limit through simple mathematical relationships. Roy and Dass (2014) formulated multiple regression models in Eqs. (2), (8) to predict shear strength parameters based on bulk density and specific gravity of soil in Sirsa, India. This study showed that bulk density and specific gravity are the two properties that have the most significant effect on the SS of soil. Adunoye (2014a, b) established quantitative relationships between cohesion, friction angle and fines content of soil samples in Eqs. (3), (4), (5), (6), (9), (10), and (11). The findings showed that the polynomial relationships are the best fit to describe these relationships. Nonetheless, identifying suitable adjustment coefficients for these equations can be a challenge, which substantially reduces the predictive accuracy (Salari *et al.* 2015, Zhu *et al.* 2022, Stefanow and Dudziński 2021).

In the era of machine learning (ML) and its application to engineering challenges, ML has evolved into a valuable tool for handling big datasets and complex conditions (Benemaran and Esmaeili-Falak 2023, Uncuoglu *et al.* 2023, Esmaeili-Falak and Benemaran 2023, Kwak and Ko 2022). There have been a large number of studies that use ML techniques to predict SS of soil, using different algorithms, especially Artificial Neural Networks (ANN) (Zhu *et al.* 2022, Chao *et al.* 2023, Chao *et al.* 2021, Pham *et al.* 2018, Iyeke *et al.* 2016, Khanlari *et al.* 2012, Mohammadi *et al.* 2022, Zakharov *et al.* 2022, Pereira *et al.* 2023). In which, Zhu *et al*. (2022) used three ML models, including Backpropagation Neural Network (BPNN), Partial Least Squares Regression, and Support Vector Regression (SVR), to predict SS of soil based on the CPT index. The findings showed that Backpropagation Neural Network proved to be one of the most suitable models for predicting the SS of soil. Similarly, Chao *et al*. (2023) integrated Backpropagation Neural Network and Mind Evolutionary Algorithm in predicting the peak shear strength of clay and confirmed that this combination is among the viable models for predicting the peak shear strength of clay. In addition, Mohammadi *et al.* (2022) made a comparison between an Artificial Neural Network model and a Multiple Linear Regression (MLR) model for shear strength prediction. The conclusion was that the ANN model produced results with greater accuracy compared to the MLR model. Besides ANN model, Support Vector Regression is another widely utilized technique for estimating the SS of soil (Zhu *et al.* 2022, Chao *et al.* 2021, Pham *et al.* 2018, Fattahi and Hasanipanah 2021). Chao *et al.* (2021) conducted a comparison between the effectiveness of the SVR model and the BPNN model in predicting the peak shear strength of soil-Geocomposite Drain Layer interfaces. The findings reveal that SVR successfully predicts the peak shear strength, although its accuracy does not exceed that of other models. A comparable result was also demonstrated in Fattahi and Hasanipanah (2021) where SVR model was used to predict the SS of rock with lower accuracy compared to Adaptive Neuro-Fuzzy Inference System. Recent studies have highlighted the effectiveness of Artificial Neural Networks and Support Vector Machine models in predicting the SS of soil. However, Ensemble Learning (EL) model and Deep Learning (DL) model, which have proven to be the robust choice and finds extensive application in addressing geotechnical engineering challenges (Nguyen and Kim 2021a, Cheng *et al.* 2021, Nguyen *et al.* 2022), has not been widely adopted for predicting shear strength parameters of soil. Presently, a multitude of distinct ML models are

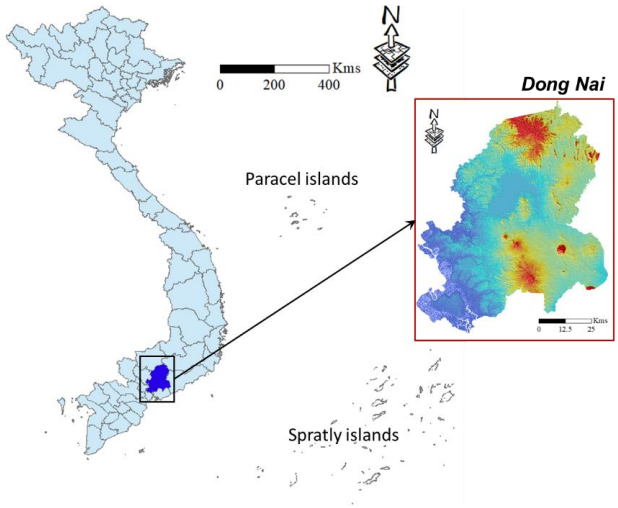

Fig. 1 Location of the study area

available, each with its unique advantages and limitations. Therefore, applying a variety of ML models for predicting the SS parameters and then selecting an appropriate ML technique are required. Furthermore, the establishment of a digital data system for engineering geological purposes in Vietnam has not received significant attention.

Building upon the above analysis, this study applied five novel ML algorithms, including Extreme Gradient Boosting (XGBoost), Random Forest (RF), Multi-layer Perceptron (MLP), Support Vector Machine (SVM), and Convolutional Neural Network (CNN) to predicting shear strength parameters, specifically cohesion and internal friction angle, based on easily-available soil physical properties. The primary goal is to furnish a straightforward and precise method for estimating these parameters across various soil types in Dong Nai province, Vietnam. The model's performance is evaluated through a comprehensive set of metrics, which include the determination coefficient (R^2), mean absolute error (MAE), and root mean square error (RMSE). Additionally, the study examines the influence of different physical properties on the model's predictive capabilities by employing the Coefficient Feature Importance (CFI), and Decision Tree Feature Importance (DTFI) techniques.

2. Study areas and data collection

Dong Nai is situated in the southeastern region of Vietnam, adjacent to Ho Chi Minh City (Fig. 1). The database is constructed from the consolidation of borehole data collected during geotechnical investigations carried out in Dong Nai province. In the survey area, the representative soil samples are extracted from each layer within the borehole. These prototypes serve as the foundation for conducting experiments to ascertain the physical and mechanical properties of the soil. The soil samples undergo testing using equipment and techniques conforming to ASTM standards. For each soil sample, every property is tested twice in parallel to ensure that the results remain within an acceptable margin of error.

A total of 332 samples were gathered from 40 boreholes in Dong Nai province and subsequently subjected to laboratory analysis to determine mechanical and physical soil properties. The observed data, encompassing cohesion and friction angle of the soil, were derived from direct shear tests conducted in accordance with ASTM standards. In addition, various physical properties of soil, namely water content (w), specific gravity (G), void ratio (e), saturation degree (S_r), plastic limit (PL), liquid limit (LL), silt content (SC), and clay content (CC), were considered as feature data for training the ML models.

3. Methods

The proposed process encompassed six distinct steps, as illustrated in Fig. 2(a). These steps are shown below:

(i) Data analysis.
(ii) Evaluation of feature correlations using Pearson and multicollinearity tests.
(iii) Division of the dataset into training (80%) and testing (20%) subsets.
(iv) Application of five ML models, including XGBoost, RF, MLP, SVM, CNN to predict shear strength parameters.
(v) Evaluation and comparative analysis of the model's performance using various metrics, including R^2, MAE, and RMSE.
(vi) Assessing feature importance using Decision Tree Feature Importance and Coefficient Feature Importance approaches.

3.1 Data analysis

Table 1 offers an initial statistical analysis of the dataset, elucidating the units for each variable. This table provides a thorough array of statistical information, encompassing the mean, standard deviation, and quantiles for observed data (Table 1(a)) and input features (Table 1(b)). Table 1a shows that the cohesion within the collected data ranges from 2.157 kPa to 41.678 kPa, with a mean value of 24.982 kPa. This indicates a wide range of cohesion suitable for most soil types. Similarly, the friction angle also falls within a suitable range, ranging from 1.833° to 26.217°.

In this study, a total of eight physical properties were considered as input features to assess cohesion and friction angle of soil. The histogram involved the evaluation of the following eight features:

Water content is a factor affecting the SS of soil (Dadkhah *et al.* 2010, Kumari 2009). Water in the soil serves a dual role, functioning both as a lubricant and a binding agent among soil particle components. This has an influence on the structural stability and strength of soil (Bláhová *et al*. 2013). In the database, water content varies from 0.112 to 0.992, and is shown in the frequency distribution in Fig. 3(a).

Specific gravity plays a crucial role in determining the SS parameter of soil. The shear strength of soil tends to increase with higher density, primarily due to a reduction in pore volume, resulting in enhanced soil resistance (García

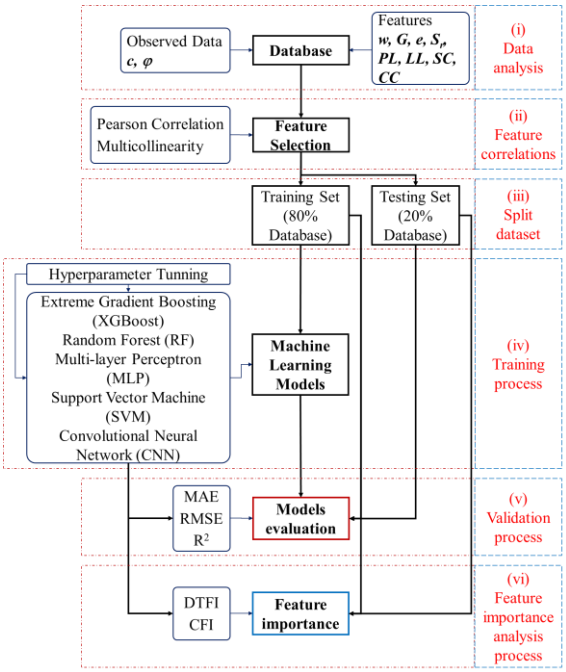

Fig. 2 (a) The flow chart of the proposed method and (b) The flow chart of the hyperparameters tuning process

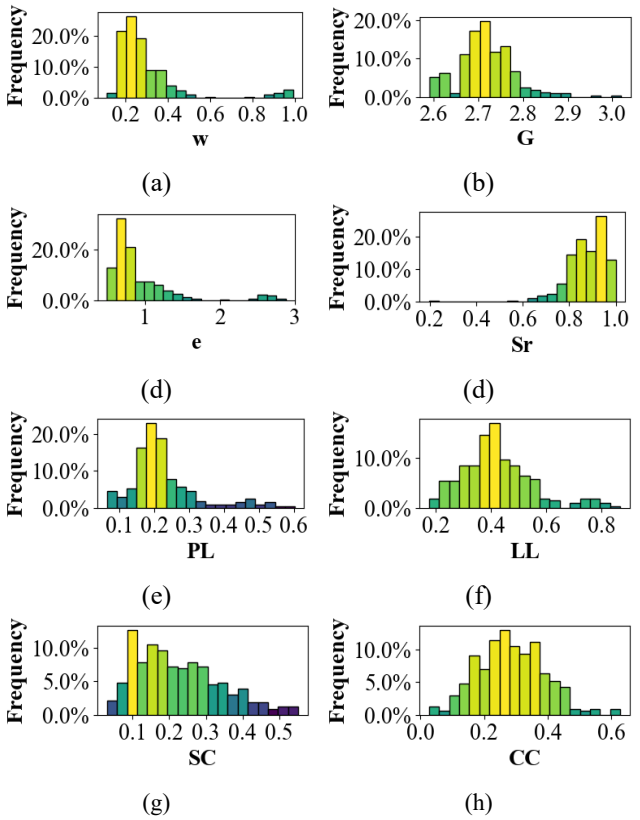

Fig. 3 Histogram of the input features

et al. 2012, Ojuri, 2013). Within the collected data, exhibits a range spanning from 2.59 to 3.02, which was mostly centered in the range 2.6-2.8 (Fig. 3(b)).

Void ratio is also a factor influencing the SS parameter of soil. In which, the friction angle increase with a decrease in void ratio (Watabe *et al.* 2017, Langfelder and Nivargikar 1967). The void ratio of soil had a range from 0.486 to 2.881, which skewed toward the smaller value ranging from 0.5 - 1.5 (Fig. 3(c)).

Degree of saturation of soil also plays a role in influencing the shear strength parameters of soil (Palani *et al.* 2020). In the field, the saturation level of soil can vary and is contingent on factors such as climatic conditions, drainage conditions, porosity, particle density, etc…There was an observation that friction angle and cohesion increase when the saturation degree decreases (Brakorenko *et al.* 2019, Yoshida *et al.* 1991). The degree of saturation varied within the range of 0.195 to 1, with a skew towards the higher values typically falling between 0.8 and 1 (Fig. 3(d)).

The Atterberg limit serves to categorize the behavior of clay into two distinct states based on water content. The plastic limit represents the water content below which the clay cannot be rolled into a thread. In contrast, the liquid limit can be defined as the state where the water content is below the point at which the clay would not flow as a liquid. Previous research has demonstrated the influence of plastic limit and liquid limit (Sharma and Bora 2003, Roman 2014, Kayabali *et al.* 2015, Roy and Dass 2014, Mousavi *et al.* 2011). In this study, the plastic limit exhibited a wide range, spanning from 0.064 to 0.603, with a bias towards lower values typically falling within the range of 0.1 to 0.3 (Fig. 3(e)). In addition, the liquid limit had a wide range extending from 0.175 to 0.867. The distribution exhibited a skew towards the lower values, typically falling within the range of 0.2 to 0.6 (Fig. 3(f)).

According to the United Soil Classification System (USCS) and the American Association of State Highway and Transportation Officials (AASHTO), fine particles are typically defined as soil particles that can pass through a sieve with a No. 200 opening, which is equivalent to 75 µm.

The researchers discovered that the friction angle exhibited a decreasing trend as the fine content increased, while the apparent cohesion displayed an increasing trend with an increase in the fine contents (Mujtaba 2014, Lade *et al.* 1998). However, it's essential to note that fines mainly

Table 1 Statistical descriptions of the database: (a) Observed data, (b) Input features

(a)

	c (kPa)	*φ (degree)*
Mean	24.982	14.986
Standard Deviation (SD)	8.660	4.863
Variance (Var)	74.988	23.653
Minimum (Min)	2.157	1.833
Maximum (Max)	41.678	26.217
Sum	8294.007	4975.480
Count	332	332

(b)

	w	*G*	*e*	S_r	*PL*	*LL*	*SC*	*CC*
Mean	0.302	2.717	0.925	0.877	0.225	0.421	0.225	0.292
SD	0.170	0.062	0.471	0.083	0.097	0.129	0.115	0.136
Var	0.029	0.004	0.221	0.007	0.009	0.017	0.013	0.019
Min	0.112	2.590	0.486	0.195	0.064	0.045	0.030	0.027
Max	0.992	3.020	2.881	1.000	0.603	0.867	0.552	1.870
Sum	100.369	902.192	307.175	291.233	74.672	139.757	74.773	96.858
Count	332	332	332	332	332	332	332	332

*w: water content, G: specific gravity, e: void ratio, S_r: degree of saturation, PL: plastic limit, LL: liquid limit, SC: silt content, CC: clay content, φ: friction angle, c: cohesion

consist of clay and silt. Therefore, this study takes into account both silt content and clay content as input features. Silt content (*SC*) varies between 0.03 and 0.552, with the majority of data falling within the range of 0.1 to 0.4, as depicted in Fig. 3(g). Furthermore, clay content (*CC*) is distributed within the range of 0.027 to 0.628, with a predominant distribution falling within the range of 0.2 to 0.4, as illustrated in Fig. 3(h).

3.2 Features correlation

3.2.1 Pearson correlation

The Pearson correlation coefficient (r) is a widely used measure for evaluating the linear correlation between features in the machine learning training process (Amin Benbouras and Petrisor 2021, Mohammadi *et al*. 2022). This coefficient, which ranges from -1 to 1, assesses both the strength and direction of the relationship between two variables. A coefficient close to 1 indicates a strong positive correlation, while a coefficient near -1 indicates a strong negative correlation. Conversely, coefficients close to zero indicate the absence of a linear correlation.

3.2.2 Multicolinearity tests

The relationships among independent features play a crucial role in data analysis and significantly affect the precision of the ML models (Arabameri *et al.* 2020, Chen and Chen 2021). Therefore, a multicollinearity test was employed in this study to evaluate the correlations among the input features. This test can identify multicollinearity issues that may lead to inaccurate results. The assessment of multicollinearity was conducted using the tolerance (TOL) and variance inflation factor (VIF)) (Nguyen and Kim 2021a, Bui *et al.* 2011). When VIF is less than 10 or TOL is greater than 0.1, these values are considered suitable for inclusion as input data (Chen *et al*. 2018).

3.3 Training and testing sets

In this study, five ML techniques were employed to predict the parameters c and φ. These ML models utilized soil physical properties (G, S_r, LL, SC, CC) as input features, while the observed data consisted of c and φ. The dataset was divided into two distinct sets: a training set, which constituted 80% of the data, and a test set, accounting for the remaining 20% of the data. The training set was used to fit and train the ML models, while the validation set was employed to evaluate the model's performance on unseen data. This division allows for an unbiased and efficient assessment of model integrity and performance. The primary purpose of the validation set is to mitigate the risk of overfitting where a model excels at predicting training data but struggles to generalize to unseen data. By evaluating the model on the validation set, we can ensure it retains the ability to make accurate predictions on new, unfamiliar samples

3.4 Machine learning models

3.4.1 Extreme gradient boosting

XGBoost is a widely recognized gradient boosting algorithm that has gained prominence in numerous

applications. It stands out as a scalable tree-boosting algorithm known for its ability to significantly enhance model efficiency (Chen and Guestrin 2016). XGBoost enhances gradient boosting algorithms through several optimizations, including parallel processing, tree-pruning, handling missing values, and regularization techniques to prevent overfitting and bias. XGBoost model involves crucial hyperparameters, such as the maximum number of trees and maximum tree depth, learning-rate, etc… These hyperparameters significantly impact the model's accuracy, performance, and computational speed (Zhang *et al*. 2021). XGBoost technique has been commonly used for solving Engineering problems (Zhang *et al*. 2021, Amjad *et al.* 2022, Shahani *et al*. 2021). Nevertheless, there is limited research on predicting soil shear strength parameters using the XGBoost model.

3.4.2 Random forest

The Random Forest algorithm is a powerful bagging learning model that incorporates numerous individual decision trees, used for constructing both regression and classification models (Cheng *et al*. 2021, Zhang *et al*. 2021). RF is widely utilized in various domains and demonstrates excellent performance (Nguyen and Kim 2021, Amjad *et al.* 2022, Zhang *et al*. 2021). RF used the bootstrap resampling method to generate multiple samples from the original dataset. It constructs a decision tree for each bootstrap sample and combines the predictions from these diverse decision trees to yield the final forecast. RF comprises some customizable parameters: the number of regression trees, the maximum depth of nodes, etc… Optimizing these parameters is essential to minimize errors in the data processing phase (Zhou *et al*. 2019, Zhang *et al*. 2021). While RF technique has found common application in solving engineering problems (Zhang *et al*. 2021, Nguyen and Kim 2021, Zhou *et al*. 2019), there is limited prior research on the prediction of soil shear strength parameters using the RF model.

3.4.3 Multi-layer perceptron

Multilayer perceptron neural network, serves as the fundamental and elementary deep neural network architecture. The MLP technique is widely recognized and applied in regression and classification tasks, particularly when substantial training data is available (Thirugnanam 2023). The MLP architecture includes an input layer responsible for receiving input data, an output layer used for predicting outcomes, and multiple hidden layers that serve as the computational core of the network. These hidden layers consist of varying numbers of neurons and are interconnected. The number of neurons in the input layer is determined by the count of selected input features. The precise number of neurons in the hidden layers and the number of training iterations are contingent on the specific training data. These values should be determined through an iterative process to achieve optimal results while preventing overfitting (Nguyen and Kim 2021, Nguyen *et al.* 2021).

3.4.4 Support vector machine

The Support Vector Machine was developed by Cortes and Vapnik (1995), and it has since become a widely-used and effective machine learning algorithm for both classification and regression problems (Nguyen and Kim 2021, Amjad *et al.* 2022, Zhong *et al.* 2010, Lee and Chern 2013). The SVM algorithm identify the optimal hyperplane within an N-dimensional space that effectively separates data points belonging to different classes in the feature space. The hyperplane is positioned in a way that maximizes the margin between the nearest points of different classes (Amjad *et al.* 2022). The kernel function type and the penalty constant value (C) are the principal parameters that significantly influence the accuracy of the SVM model (Nguyen and Kim 2021).

3.4.5 Convolutional Neural Network

Convolutional Neural Network is one of the most powerful deep learning architecture (LeCun *et al.* 2015) known for their strong performance in object detecting and classification (Girshick 2015). A typical CNN model is a variant of a multilayer perceptron that includes an input layer, one or more convolutional layers, max pooling layers, fully connected layers, and an output layer (Shin *et al.* 2016). The input layer consists of the input features for training. The convolutional layers are designed to extract various features from the input layer (Razavian *et al.* 2014) and include filters and feature maps (Sharif Razavian *et al.* 2014, Brownlee 2016). Each convolutional filter, also known as a neuron or kernel, is a two-dimensional matrix that slides across the previous layer to produce a feature map, representing the output of one filter applied to that layer. The number and size of the kernels in these layers significantly impact the performance of the CNN model. Pooling is a technique used for downsampling to reduce the dimensionality of the feature maps (Brownlee 2016, Wang *et al.* 2019). It helps to compress or generalize feature maps, generally reducing the risk of overfitting during training (Brownlee 2016). Max pooling, a common pooling method, condenses the feature maps by sliding a 2×2 matrix over each feature map and retaining the maximum value at each position. In the fully connected layer, the 2D feature maps are flattened into a traditional fully connected format (Brownlee 2016). The number of neurons in this layer is carefully chosen to achieve optimal results. The output layer generates results that allow for predicting the SS parameters.

3.4.6 Hyperparameter tuning

In ML, hyperparameters are parameters that must be predefined before the learning process. XGBoost, RF, MLP, SVM, and CNN models are influenced by various hyperparameters that significantly affect their predictive accuracy. Hence, it is crucial to perform careful tuning of these hyperparameters, a process known as hyperparameter optimization. However, optimizing hyperparameters poses a challenge because it involves combinatorial optimization, which cannot be handled by gradient descent methods as with regular parameters. Furthermore, individually adjusting hyperparameters and evaluating their impact requires retraining, making the computation for assessing various hyperparameter configurations a computationally intensive task (Zhang *et al.* 2021). Hence, Bayesian optimization, in conjunction with K-fold cross-validation, was employed to reduce the computational demands associated with hyperparameter optimization. Bayesian optimization involves two key components: a surrogate

model representing the ML model, which defines the prior probability, and an acquisition function (a function of posterior probability) for guiding the next evaluation. The K-fold cross-validation process divides the training set into k subsets referred to as folds. Subsequently, the models under examination are trained and evaluated k times. During each iteration, k-1 folds are used for training, and the remaining fold is reserved for evaluating the classification model. The outcomes of K-fold cross-validation are represented as an array containing k evaluation scores (Xia *et al.* 2017). The flowchart of the tuning of hyperparameters using K-fold validation and Bayesian optimization algorithm was shown in Fig. 2(b).

3.5 Model performance assessment

To evaluate the predictive performance of the ML models, three commonly accepted validation criteria were selected and utilized: the coefficient of determination (R^2), Mean Absolute Error (MAE), and Root Mean Squared Error (RMSE) (Chao *et al.* 2021, Pham *et al.* 2018, Khanlari *et al.* 2012, Zhang *et al.* 2021). R^2 represents the statistical relationship between the observed values and the predicted values generated by the models (Mohammadi *et al.* 2022). Its values fall within the range of 0 to 1, where 0 indicates an inaccurate model and 1 indicates a highly accurate model (Zhang *et al.* 2021). On the other hand, MAE calculates the mean of the absolute differences between the predicted and observed values (Khanlari *et al.* 2012). While, RMSE quantifies the average squared difference between observed and predicted values (Khanlari *et al.* 2012). Both MAE and RMSE provide insights into the model's error assessment, with lower values indicating better model performance (Zhang *et al.* 2021). These values (R^2, MAE, RMSE) can be calculated using the following equations.

$$R^2 = 1 - \frac{\sum_{i=1}^{n}(Y_i - X_i)^2}{\sum_{i=1}^{n}(Y_i - \bar{Y})^2} \quad (12)$$

$$MAE = \frac{1}{n}\sum_{i=1}^{n}|Y_i - X_i| \quad (13)$$

$$RMSE = \sqrt{\frac{1}{n}\sum_{i=1}^{n}(Y_i - X_i)^2} \quad (14)$$

where, Y_i is measured value, X_i is predicted value, $\bar{Y}$ is the average of measured value, and n is data numbers.

3.6 Feature importance assessment techniques

Feature importance is a vital aspect for feature selection and model interpretation. In this study, the Decision Tree Feature Importance (DTFI) and Coefficient Feature Importance (CFI) techniques were employed to assess the contributions and importance levels of the input features in predicting cohesion and friction angle. The DTFI method yields importance scores for the input features, which are computed using the Gini impurity. Gini impurity measures how effectively observations can be divided based on the target variable at each node in the decision tree. While, the CFI identifies a set of coefficients used in a weighted sum to make predictions. These coefficients can be directly utilized as a fundamental form of feature importance score.

Table 2 Pearson's correlation coefficients

	w	*G*	*e*	S_r	*PL*	*LL*	*SC*	*CC*
w	1							
G	-0.299	1						
e	**0.986**	-0.213	1					
S_r	0.265	-0.175	0.144	1				
PL	**0.845**	-0.167	**0.828**	0.315	1			
LL	**0.831**	0.081	**0.837**	0.306	**0.824**	1		
SC	0.309	-0.169	0.279	0.275	0.408	0.311	1	
CC	0.291	-0.019	0.257	0.318	0.312	0.517	0.415	1

Table 3 Multicollinearity test results

Features	VIF	TOL
G	1.10	0.91
S_r	1.20	0.84
LL	1.36	0.73
SC	1.22	0.82
CC	1.27	0.79

4. Results and discussions

4.1 Selecting features

4.1.1 Pearson correlation

Table 2 illustrate Pearson's correlation coefficients, which reveal the relationships among various soil physical properties. Specifically, the correlation coefficients between water content (*w*), void ratio (*e*), plastic limit (*PL*), and liquid limit (*LL*) exhibit a notably high range, spanning from 0.824 to 0.986, signifying a statistically significant positive correlation. The presence of highly correlated input features can potentially impair the performance of ML algorithms. To ensure the optimal performance of the model, these closely related input features will be assessed for potential removal from the dataset due to their significant similarity to one another, as indicated in prior research of Mohammadi *et al.* (2022). Consequently, water content, void ratio, and plastic limit will be excluded from the input features used in the ML models.

4.1.2 Multicollinearity test

After removing the three input features, a multicollinearity test was conducted on the remaining features to examine their correlations with one another. The findings of this assessment are summarized in Table 3. This table confirms that all the features exhibit no signs of multicollinearity, as indicated by the variance inflation factor (VIF) values ranging from 1.10 to 1.36 and tolerance (TOL) values ranging from 0.73 to 0.91.

Table 4 Hyperparameter selection

XGBoost	
Hyperparameters	Value
n_estimators	600
Max_depth	4
Learning_rate	0.036
Colsample_bytree	0.5
Subsample	0.3
Reg_lambda	0.1
RF	
Hyperparameters	Value
n_estimators	1000
Max_depth	7
Bootstrap	True
Min_samples_leaf	1
Min_samples_split	2
MLP	
Hyperparameters	Value
Epochs	5000
Batch_size	10
Activation function	Sigmoid
Optimizer model	Adam
Hidden layer	2
Neurons in hidden layer	10, 5
SVM	
Hyperparameters	Value
Kernel function	rbf
C	100
Gamma	10
CNN	
Hyperparameters	Value
Convolutional layers	
Number of convolutional layer	2
Number of kernels	64; 32
Size of kernels	4
Activation function	RELU
Fully connected layers	
Number of fully connected layers	3
Number of neurons	256; 128; 1
Activation function	Linear
Batch size	10
Epochs	5000
Optimizer model	Adam

4.2 Hyperparameter selection

Table 4 displays the hyperparameters selected for the ML models through K-fold validation and Bayesian optimization method. The specific hyperparameters for XGBoost, RF, MLP, SVM, and CNN can be found in Table 4.

4.3 Shear strength parameters prediction

Fig. 4 displays the comparison between cohesion observations and predictions using the training and testing dataset, visualized alongside the trend line. The data is closely clustered around the trend line, indicating a strong correlation as evidenced by the high R^2 value. The R^2 values for the training and validation datasets of XGBoost, RF, MLP, SVM, and CNN were illustrated in Figs. 4a-4(e) respectively. These R^2 values, which fell within the range of 0.770 to 0.982, clearly indicate the success of all the applied machine learning techniques in accurately estimating the soil cohesion. Among the used ML models, XGBoost and CNN exhibit the highest performance in comparison to the other models (Fig. 4(f)).

Similar to Figs. 4 and 5 illustrates the comparison between observed friction angle values and their predictions using both the training and testing datasets, with a trend line

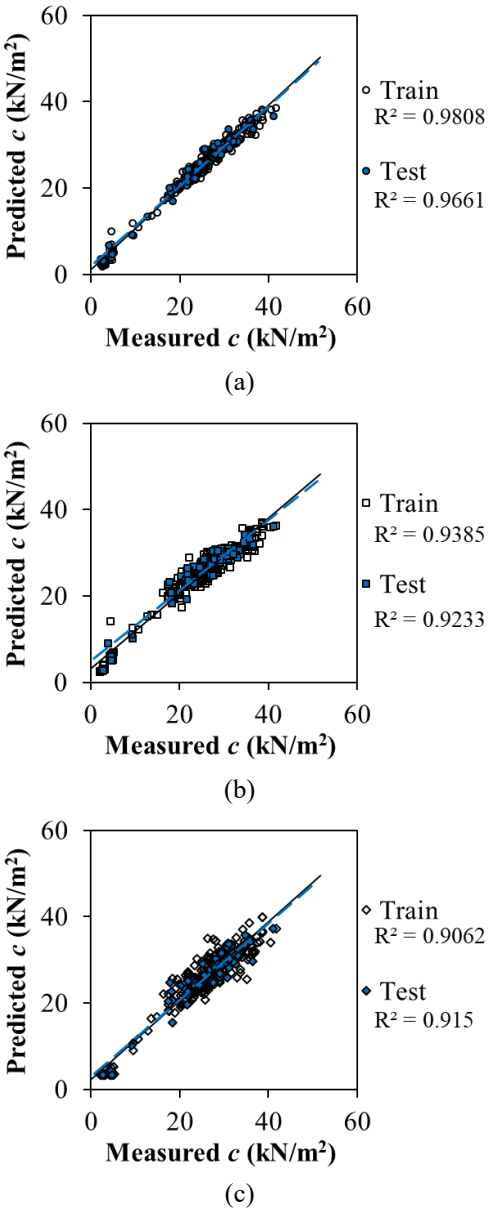

Fig. 4 Correlation between the measured and predicted cohesion: (a) XGBoost, (b) RF, (c) MLP, (d) SVM, (e) CNN and (f) Comparison of R^2 among ML models

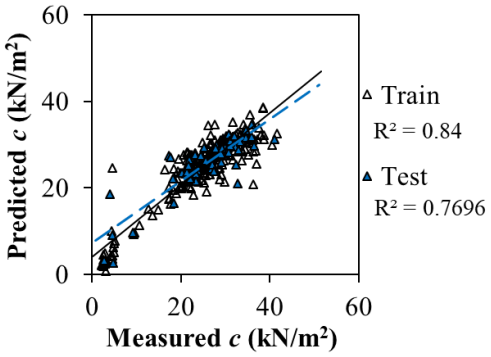

(d)

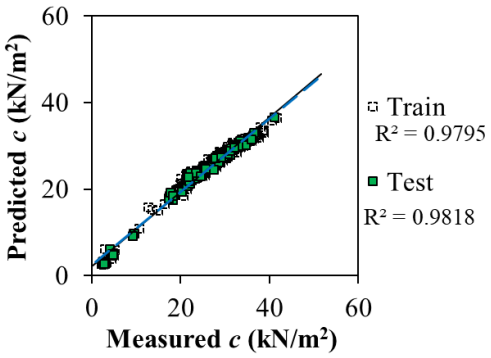

(e)

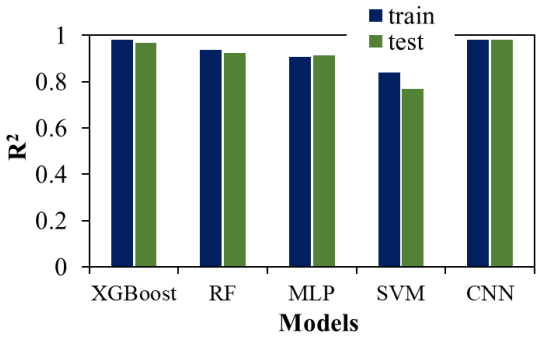

(f)

Fig. 4 Continued-

for reference. Figs. 5(a)-5(e) show the R^2 values for the training and validation datasets of XGBoost, RF, MLP, SVM, and CNN respectively. The R^2 values, ranging from 0.877 to 0.987, affirm the effectiveness of all employed machine learning techniques in precisely predicting soil friction angle. Notably, Fig. 5(f) compares R^2 values among the ML models. The result also confirmed the superior prediction ability of XGBoost and CNN techniques compared to other used models.

Fig. 6 presents the MAE and RMSE values in cohesion prediction from the used ML models for both the training and testing datasets. Regarding both MAE (as shown in Fig. 6(a)) and RMSE (as depicted in Fig. 6b), the XGBoost model exhibits the highest accuracy in comparison to the other techniques. Moreover, the prediction performance of CNN, RF and MLP is quite similar, while SVM demonstrates the least favorable model performance. In similarity, Fig. 7 displays the MAE and RMSE values for friction angle prediction derived from the employed ML models, encompassing both the training and validating

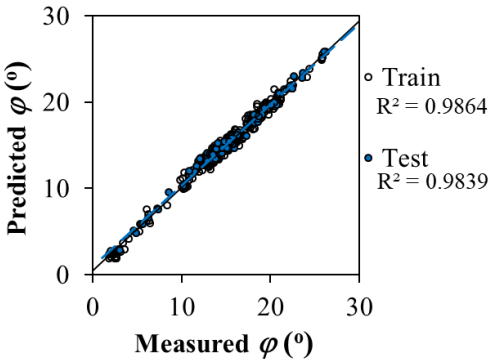

(a)

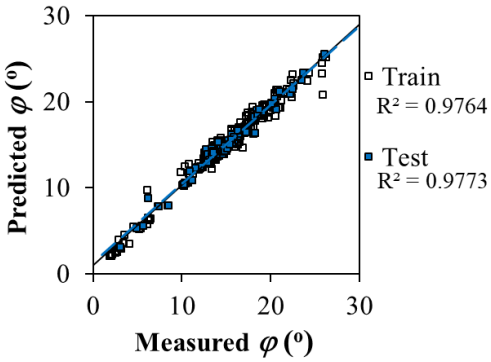

(b)

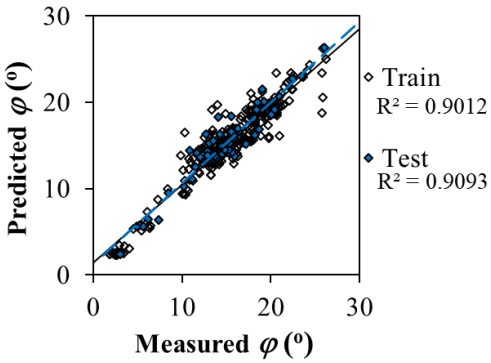

(c)

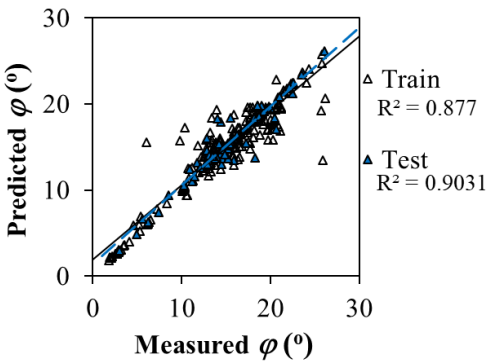

(d)

Fig. 5 Correlation between the measured and predicted friction angle: (a) XGBoost, (b) RF, (c) MLP, (d) SVM, (e) CNN and (f) Comparison of R^2 among ML models

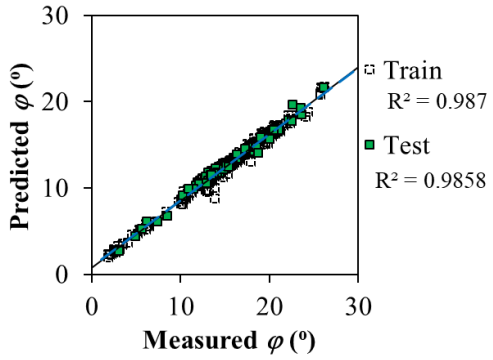

(e)

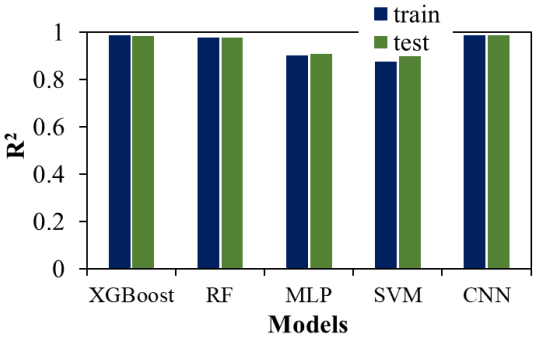

(f)

Fig. 5 Continued-

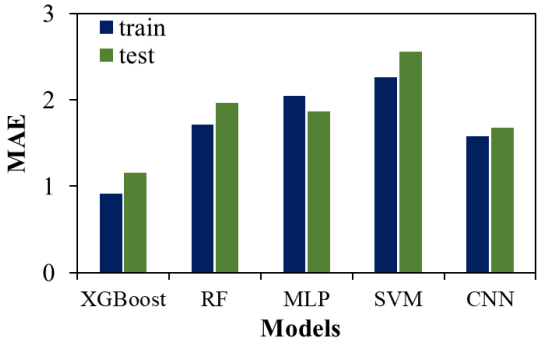

(a)

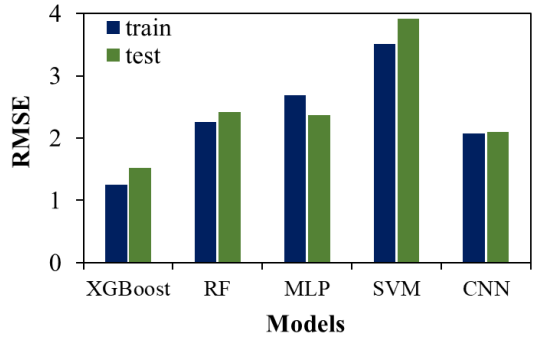

(b)

Fig. 6 Comparison among the ML models cohesion prediction: (a) MAE and (b) RMSE

datasets. The XGBoost model displays the lowest MAE and RMSE values compared to the other three models. CNN, and RF shows slightly higher MAE and RMSE values than

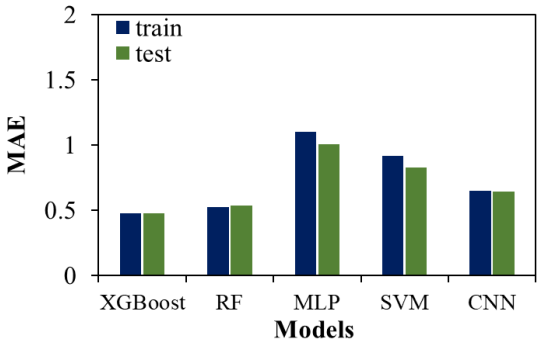

(a)

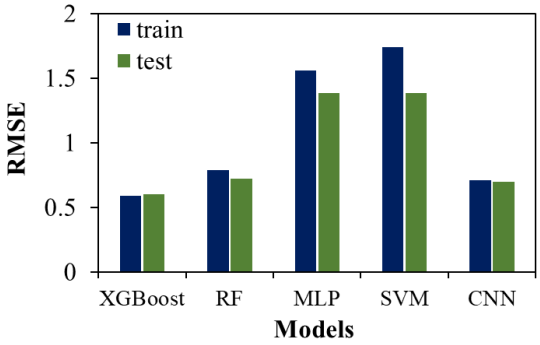

(b)

Fig. 7 Comparison among the ML models friction angle prediction: (a) MAE and (b) RMSE

XGBoost, while MLP and SVM exhibit the highest values for both MAE and RMSE.

In Fig. 8(a), the probability density distribution curve for observed cohesion and predicted cohesion from the various ML models is depicted.

4.4 Selecting appropriate ML models

The results from Figs. 4-8 clearly suggest that the XGBoost model exhibited the best performance in predicting the SS parameters of soil. This discovery is in line with findings from previous studies, which proved the outstanding predictive ability of XGBoost model for solving the engineering problems. Kulsoom *et al.* (2023), Sahin (2020), Inan and Rahman (2023) demonstrated that XGBoost model exhibited the highest level of accuracy when compared to the RF, ANN, SVM, and AdaBoost for landslide prediction. Amjad *et al.* (2022) illustrated the superior predictive capabilities of XGBoost when compared to RF, SVM, and Decision Tree in estimating pile bearing capacity.

The exceptional performance of the XGBoost model arises from its training process, which involves the sequential training of multiple decision trees. Each decision tree is relatively shallow and fine-tuned using the errors from the previous tree. This approach generates numerous weak classifiers that, when combined, result in a highly effective model (Inan and Rahman 2023). CNN model is recognized as one of the most effective deep learning algorithms for image classification problems (Lei *et al.* 2019, Chaganti *et al.* 2020, Tripathi 2021, Guo *et al.* 2017).

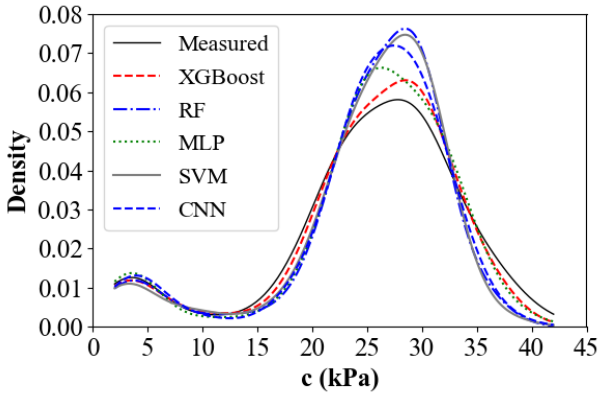

(a)

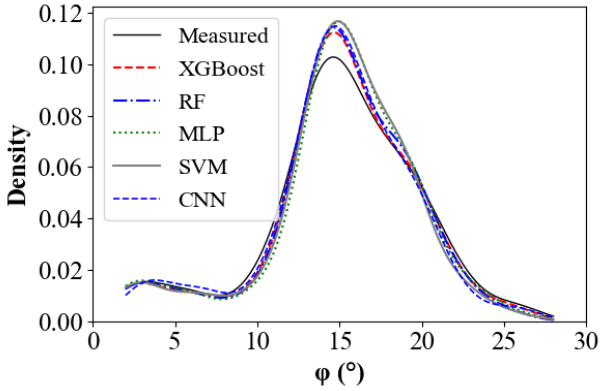

(b)

Fig. 8 Comparison of probability distribution curve between the observed data and the ML models: (a) cohesion and (b) friction angle

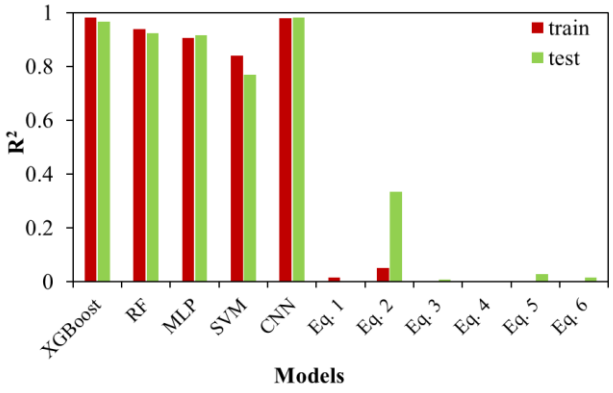

(a)

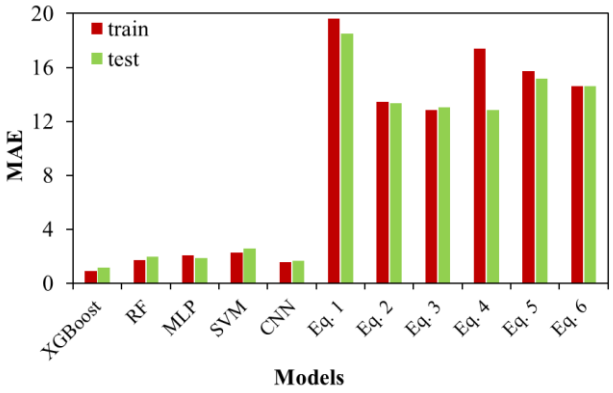

(b)

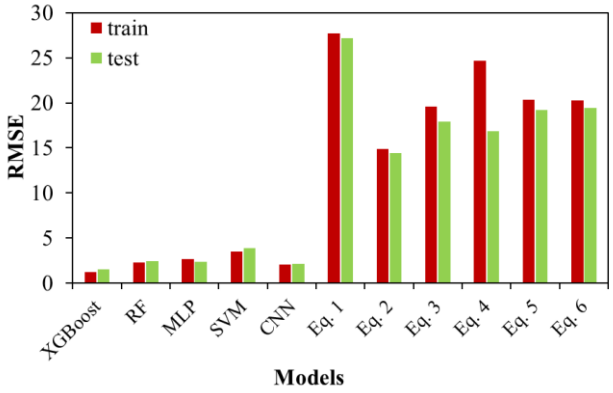

(c)

Fig. 9 Comparison between this study and the previous studies for cohesion prediction: (a) R^2, (b) MAE and (c) RMSE

However, in the context of regression problems, such as in this study, while the R^2 value is comparable to that of the XGBoost model, the MAE and RMSE error metrics are higher for the CNN model. This discrepancy arises from the process of transforming the input data from continuous to categorical (converting vectors to 2-dimensional matrices). Although adding more classification layers in the transformation of the input data can help reduce errors in the predicting using CNN model, it also leads to increased computation time. Consequently, for regression problems, the XGBoost model appears to be a more suitable choice than the CNN model.

The comparatively lower performance observed in the RF model, when compared to XGBoost, can be attributed to the RF model's heavier reliance on hyperparameters to optimize its performance. Consequently, even a minor alteration in hyperparameters can have a far-reaching effect on most trees within the RF ensemble, potentially influencing its predictive accuracy. These challenges can erode the effectiveness of the RF model, whereas XGBoost consistently focuses on optimizing the model's functional space while minimizing associated costs, leading to improved performance (Probst *et al*. 2019, Kulsoom *et al.* 2023). The relatively lower performance of the MLP model, compared to the XGBoost and RF models, can be attributed to the inherent challenge faced by MLP models in effectively generalizing from training data. This challenge can lead to issues such as overfitting, where the model fits the training data too closely, resulting in reduced performance when applied to new data (Bandara *et al*. 2020, Kulsoom *et al*. 2023). The lower performance of the SVM model, compared to the other used models, can come from the nature of SVM. SVM is a linear separator, and when dealing with non-linearly separable data, SVM relies on the use of a Kernel to transform the data into a space where it can be effectively separated. Although SVM has the capability to project data into a high-dimensional space to identify a linear separation for various types of data, it's

important to note that the effectiveness of SVM depends on selecting an appropriate Kernel. However, it's worth acknowledging that there might not always be a perfect Kernel choice for every dataset (Ates *et al.* 2021, Karamizadeh *et al.* 2014). Out of the ML models assessed in this study, it is evident that the XGBoost model stands out as the most appropriate choice for predicting the SS parameters of soil.

4.5 Comparison with the previous researches

To gauge the effectiveness of the ML models, the prediction ability from five ML techniques was compared to the empirical equations (Eqs. (1)-(11)) from four studies proposed by Ersoy *et al.* (2013); Roy and Dass (2014), Adunoye (2014a); Adunoye, (2014b). The reason for this selection is that the dataset used in this study contains most of the required parameters for calculating shear strength parameters using these equations.

The performance of both the empirical methods and the used ML models on the training and validation sets is illustrated in Figs. 9 and 10, focusing on cohesion and friction angle, respectively. In the context of predicting cohesion (as shown in Fig. 9), the employed models consistently exhibits higher R^2 values when compared to the previously used empirical equations, both for the training and testing datasets (as depicted in Fig. 9(a)). Furthermore, it's worth noting that the ML techniques display lower MAE (as seen in Fig. 9(b)) and RMSE (as demonstrated in Fig. 9(c)) values in comparison to the previous empirical formulas. These findings are similarly consistent when predicting the friction angle, as illustrated in Fig. 10. These results emphasize the superior predictive capabilities of the ML models when compared to the previous empirical models. This observation can be explained as follows: the previous empirical equations were derived using a linear regression approach. This technique assumes linearity between the features, potentially leading to less accurate results (Iyeke *et al.* 2016).

Moreover, this method may lead to an overfitting issue, causing excessive similarities between the analysis and the dataset, and potentially resulting in unreliable predictions and inaccurate future forecasts. Finally, the previous empirical equations relied on one or two soil physical properties to predict the SS parameters of soil. Each study used different properties, such as Ersoy *et al.* (2013) used plastic and liquid limits; Roy and Dass, (2014) used bulk density and specific gravity; Adunoye, (2014a) used fine content, to predict the SS parameters and concluded that the identified properties significantly influence the SS parameters. This underlines the complexity of SS, indicating its dependence on different physical soil properties (Jain *et al.* 2010, Mousavi *et al.* 2011). Therefore, predicting the SS parameters requires models that take into account the influence of various properties.

4.6 Features importance analysis

The importance of the input parameters for predicting cohesion and friction angle is depicted in Fig. 11. In both the DTFI and CFI analyses, it is evident that *G* and *LL* have a substantial impact on cohesion (Fig. 11(a)) and friction angle (Fig. 11(b)). These findings are suitable to the researches of (García *et al.* 2012, Ojuri 2013), which presented an increase in soil density typically leads to an enhancement in shear strength, mainly due to a reduction in pore volume. In a similar way, shear strength parameters tend to increase with an increase in the liquid limit (Sharma and Bora 2003, Roman, 2014, Kayabali *et al.*2015, Roy and Dass 2014, Mousavi *et al.* 2011). Furthermore, SC and CC also exert an influence on cohesion and friction angle in

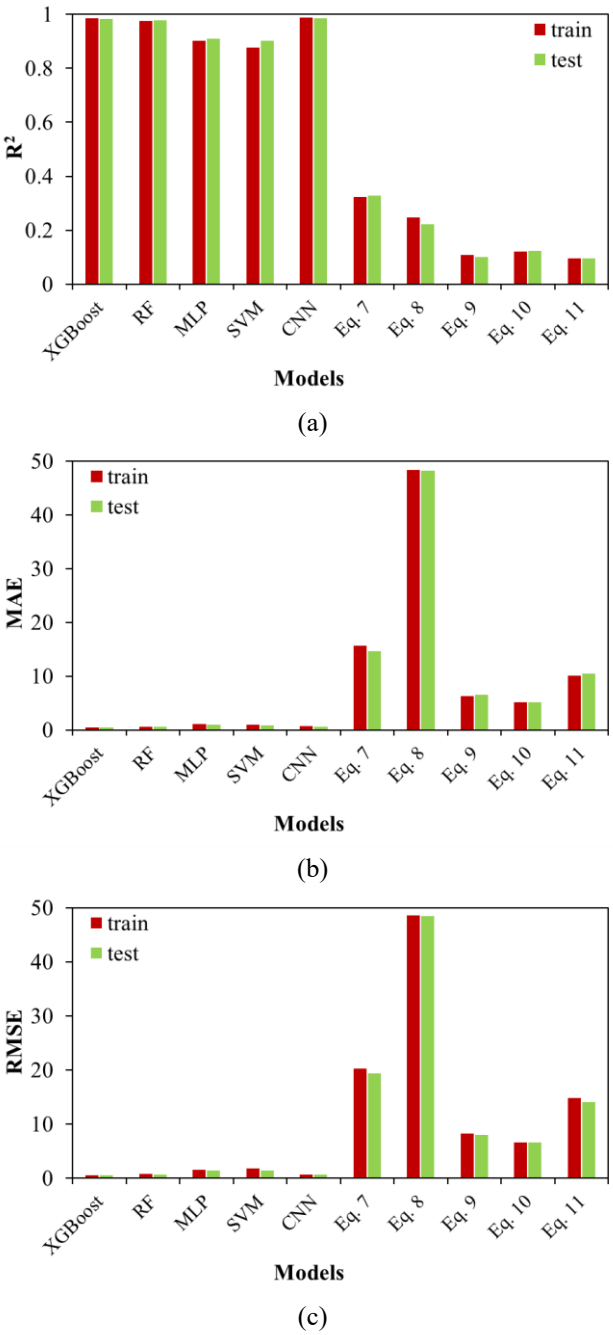

Fig. 10 Comparison between this study and the previous studies for friction angle prediction: (a) R^2, (b) MAE and (c) RMSE

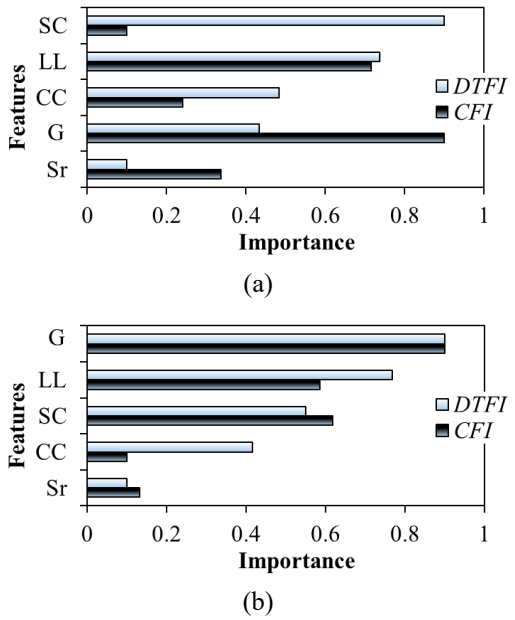

Fig. 11 Importance of the input features: (a) cohesion and (b) friction angle

both the DTFI and CFI methods. This observation presented in the studies of Mujtaba (2014), Lade *et al.* (1998), Adunoye (2014a, b). These researches revealed that the friction angle showed a decreasing trend with an increase in fine content, whereas the cohesion displayed an increasing trend as fine content increased.

This can be explained as follows: as the silt content increases, resulting in increased density and decreased void ratio, soil water exists predominantly in the form of a binding membrane around the soil particles. In this state, the water inside the binding membrane is immobile, which facilitates the surface tension of water in the soil. As a result, the increased density leads to a strong binding force between the water in the water membrane and the soil particles, which contributes to a certain extent of cohesion increase (Li *et al*. 2021). Fig. 11 estimates that the influence of S_r is quite low compared to the other properties, which may come from the fact that the S_r data used to train the ML models is mainly in the range of 0.8-1.0. This limited range of S_r values results in a marginal impact of S_r on the ML model's performance.

5. Conclusions

This study investigates the applicability of the XGBoost, RF, MLP, SVM, and CNN models for predicting the SS parameters, including cohesion and friction angle. To evaluate the model's performance, the study utilizes metrics including R^2 (coefficient of determination), MAE (mean absolute error), and RMSE (root mean square error). The results of these metrics demonstrate that the used ML techniques effectively predict shear strength parameters based on readily available physical properties. The evaluation results further validate the superior performance of the XGBoost model, establishing it as one of the most suitable models for accurately estimating both cohesion and friction angle.

The results obtained from this study were compared with those from previous empirical equations, revealing the superior predictive capability of the ML models in estimating shear strength parameters.

The influence of input features on the prediction outcomes was also evaluated using the Decision Tree Feature Importance, and Coefficient Feature Importance methods. The results from these methods suggest that *G* and *LL* exert significant influence on the prediction of cohesion and friction angle. In addition, both silt content and clay content also have an impact on the shear strength parameters.

Acknowledgements

This research is funded by Vietnam National University Ho Chi Minh City (VNU-HCM) under grant number C2023-28-07.

References

Adunoye, G.O. (2014a), "Fines content and angle of internal friction of a lateritic soil: an experimental study", *Am. J. Eng. Res.*, **3**(3), 16-21.

Adunoye, G.O. (2014b), "Study of relationship between fines content and cohesion of soil", *British J. Appl. Sci. Technol.*, **4**(4), 682-692. https://doi.org/10.9734/BJAST/2014/6290.

Amin Benbouras, M. and Petrisor, A.I. (2021), "Prediction of swelling index using advanced machine learning techniques for cohesive soils", *Appl. Sci.*, **11**(2), 536. https://doi.org/10.3390/app11020536.

Amjad, M., Ahmad, I., Ahmad, M., Wróblewski, P., Kamiński, P., and Amjad, U. (2022), "Prediction of pile bearing capacity using XGBoost algorithm: Modeling and performance evaluation", *Appl. Sci.*, **12**(4), 2126. https://doi.org/10.3390/app12042126.

Arabameri, A., Saha, S., Roy, J., Chen, W., Blaschke, T. and Tien Bui, D. (2020), "Landslide susceptibility evaluation and management using different machine learning methods in the Gallicash River Watershed, Iran", *Remote Sens.*, **12**(3), 475. https://doi.org/10.3390/rs12030475.

Ates, E.C., Bostanci, E. and Guzel, M.S. (2021), "Comparative performance of machine learning algorithms in cyberbullying detection: Using turkish language preprocessing techniques", *ArXiv:2101.12718*. https://doi.org/10.48550/arXiv.2101.12718.

Bandara, A., Hettiarachchi, Y., Hettiarachchi, K., Munasinghe, S., Wijesinghe, I. and Thayasivam, U. (2020), "A generalized ensemble machine learning approach for landslide susceptibility modeling", *Data Management, Analytics and Innovation: Proceedings of ICDMAI 2019*, **2**, 71-93.

Benemaran, R.S. and Esmaeili-Falak, M. (2023), "Predicting the Young's modulus of frozen sand using machine learning approaches: State-of-the-art review", *Geomech. Eng.*, **34**(5), 507-527. https://doi.org/10.12989/gae.2023.34.5.507.

Bláhová, K., Ševelová, L. and Pilařová, P. (2013), "Influence of water content on the shear strength parameters of clayey soil in relation to stability analysis of a hillside in Brno region", *Acta Universitatis Agriculturae et Silviculturae Mendelianae Brunensis*, **61**(6), 1583-1588. https://doi.org/10.11118/actaun201361061583.

Brakorenko, N., Leonova, A. and Nikitenkov, A. (2019), "Effect of soil water saturation on slope stability: Tomsk case study", *E3S Web of Conferences*, **98**, 5005.

Brownlee, J. (2016), *Deep learning with python: Develop deep learning models on theano and tensorflow using keras*. Machine Learning Mastery.

Bui, D.T., Lofman, O., Revhaug, I. and Dick, O. (2011), "Landslide susceptibility analysis in the Hoa Binh province of Vietnam using statistical index and logistic regression", *Nat. Hazards*, **59**(3), 1413. https://doi.org/10.1007/s11069-011-9844-2.

Chaganti, S.Y., Nanda, I., Pandi, K.R., Prudhvith, T.G. and Kumar, N. (2020), "Image Classification using SVM and CNN", *Proceedings of the 2020 International Conference on Computer Science, Engineering and Applications (ICCSEA)*.

Chao, Z., Fowmes, G. and Dassanayake, S.M. (2021), "Comparative study of hybrid artificial intelligence approaches for predicting peak shear strength along soil-geocomposite drainage layer interfaces", *Int. J. Geosynth. Ground Eng.*, **7**(3), 60. https://doi.org/10.1007/s40891-021-00299-2.

Chao, Z., Shi, D., Fowmes, G., Xu, X., Yue, W., Cui, P., Hu, T., and Yang, C. (2023), "Artificial intelligence algorithms for predicting peak shear strength of clayey soil-geomembrane interfaces and experimental validation", *Geotext. Geomembranes*, **51**(1), 179-198. https://doi.org/10.1016/j.geotexmem.2022.10.007.

Chen, T. and Guestrin, C. (2016). "Xgboost: A scalable tree boosting system", *Proceedings of the 22nd Acm Sigkdd International Conference on Knowledge Discovery and Data Mining*.

Chen, W., Zhang, S., Li, R. and Shahabi, H. (2018). "Performance evaluation of the GIS-based data mining techniques of best-first decision tree, random forest, and naïve Bayes tree for landslide susceptibility modeling", *Sci. Total Environ.*, **644**, 1006-1018. https://doi.org/10.1016/j.scitotenv.2018.06.389.

Chen, X. and Chen, W. (2021). "GIS-based landslide susceptibility assessment using optimized hybrid machine learning methods", *Catena*, **196**, 104833. https://doi.org/10.1016/j.catena.2020.104833.

Cheng, Y.S., Yu, T.T. and Son, N.T. (2021), "Random forests for landslide prediction in tsengwen river watershed, central taiwan", *Remote Sens.*, **13**(2), 199. https://doi.org/10.3390/rs13020199.

Chitra, R. and Gupta, M. (2014), "Neural networks for assessing shear strength of soils", *Int. J. Recent Dev. Eng. Technol.*, **3**(4), 24-32.

Cortes, C. and Vapnik, V. (1995), "Support-vector networks", *Machine Learning*, **20**, 273-297.

Dadkhah, R., Ghafoori, M., Ajalloeian, R. and Lashkaripour, G.R. (2010), "The effect of scale direct shear tests on the strength parameters of clayey sand in Isfahan city, Iran", *J. Appl. Sci.*, *18*. DOI: 10.3923/jas.2010.2027.2033.

Ersoy, H., Karsli, M.B., Cellek, S., Kul, B., Baykan, I. and Parsons, R.L. (2013). "Estimation of the soil strength parameters in Tertiary volcanic regolith (NE Turkey) using analytical hierarchy process", *J. Earth Syst. Sci.*, **122**, 1545-1555. https://doi.org/10.1007/s12040-013-0366-z

Esmaeili-Falak, M. and Benemaran, R.S. (2023), "Ensemble deep learning-based models to predict the resilient modulus of modified base materials subjected to wet-dry cycles", *Geomech. Eng.*, **32**(6), 583–600. https://doi.org/10.12989/gae.2023.32.6.583.

Fattahi, H. and Hasanipanah, M. (2021). "Predicting the shear strength parameters of rock: A comprehensive intelligent approach", *Geomech. Eng.*, **27**(5), 511. https://doi.org/10.12989/gae.2021.27.5.511.

García, A.J.H., Jaime, Y.N.M., Contreras, Á.M.Z., Bastardo, L.D. S. and Llovera, F.A.S. (2012). "Savanna soil water content effect on its shear strength-compaction relationship", *Revista Científica UDO Agrícola*, **12**(2), 324-337.

Girshick, R. (2015), "Fast r-cnn. *Proceedings of the IEEE International Conference on Computer Vision*, 1440-1448.

Goktepe, A.B., Altun, S., Altintas, G. and Tan, O. (2008), "Shear strength estimation of plastic clays with statistical and neural approaches", *Build. Environ.*, **43**(5), 849-860. https://doi.org/10.1016/j.buildenv.2007.01.022.

Guo, T., Dong, J., Li, H. and Gao, Y. (2017), "Simple convolutional neural network on image classification", *Proceedings of the 2017 IEEE 2nd International Conference on Big Data Analysis (ICBDA)*.

Hosseini, M., Movahedi Naeini, S.A.R., Dehghani, A.A. and Zeraatpisheh, M. (2018), "Modeling of soil mechanical resistance using intelligent methods", *J. Soil Sci. Plant Nutrition*, **18**(4), 939-951. https://doi.org/10.4067/S0718-95162018005002702.

Inan, M.S.K. and Rahman, I. (2023), "Explainable AI integrated feature selection for landslide susceptibility mapping using TreeSHAP", *SN Comput. Sci.*, **4**(5), 482. https://doi.org/10.1007/s42979-023-01960-5.

Iyeke, S.D., Eze, E.O., Ehiorobo, J.O. and Osuji, S.O. (2016), "Estimation of shear strength parameters of lateritic soils using artificial neural network", *Nigerian J. Technol.*, **35**(2), 260-269. https://doi.org/10.4314/njt.v35i2.5.

Jain, R., Jain, P.K. and Bhadauria, S.S. (2010), "Computational approach to predict soil shear strength", *Int. J. Eng. Sci. Tech.*, **2**(8), 3874-3885.

Karamizadeh, S., Abdullah, S.M., Halimi, M., Shayan, J. and javad Rajabi, M. (2014), "Advantage and drawback of support vector machine functionality", *Proceedings of the 2014 International Conference on Computer, Communications, and Control Technology (I4CT)*.

Kayabalı, Ö., Aktürk, M., Fener, A.B., Üstün, O., Dikmen, O. and Harputlugil, F.H. (2015), "Evaluation of undrained shear strength of fine-grained soils in consideration of soil plasticity", *Yerbilimleri*, **36**(3), 121-136. https://doi.org/10.17824/yrb.99784.

Khanlari, G.R., Heidari, M., Momeni, A.A. and Abdilor, Y. (2012), "Prediction of shear strength parameters of soils using artificial neural networks and multivariate regression methods", *Eng. Geol*., **131**, 11-18. https://doi.org/10.1016/j.enggeo.2011.12.006.

Kulsoom, I., Hua, W., Hussain, S., Chen, Q., Khan, G. and Shihao, D. (2023), "SBAS-InSAR based validated landslide susceptibility mapping along the Karakoram Highway: A case study of Gilgit-Baltistan, Pakistan", *Scientific Reports*, **13**(1), 3344. https://doi.org/10.1038/s41598-023-30009-z.

Kumari, D. (2009), *A study on the effect of moisture on strength characteristics of river sand*.

Kwak, N.S. and Ko, T.Y. (2022), "Machine learning-based regression analysis for estimating Cerchar abrasivity index", *Geomech. Eng.*, **29**(3), 219-228. https://doi.org/10.12989/gae.2022.29.3.219.

Lade, P.V., Liggio, C.D. and Yamamuro, J.A. (1998), "Effects of non-plastic fines on minimum and maximum void ratios of sand", *Geotech. Test. J.*, **21**, 336-347. https://doi.org/10.1520/GTJ11373J.

Langfelder, L.J. and Nivargikar, V.R. (1967), "Some factors influencing shear strength and compressibility of compacted soils", *Highway Res. Record*, 177.

LeCun, Y., Bengio, Y. and Hinton, G. (2015), "Deep learning", *Nature*, **521**(7553), 436.

Lee, C.Y. and Chern, S.G. (2013), "Application of a support vector machine for liquefaction assessment", *J. Mar. Sci. Tech.*, **21**(3), https://doi.org/10.6119/JMST-012-0518-3.

Lei, X., Pan, H. and Huang, X. (2019), "A dilated CNN model for image classification", *IEEE Access*, *7*, 124087-124095.

https://doi.org/10.1109/ACCESS.2019.2927169.

Li, J., Geng, H., Zhang, G. and Jin, G. (2021), "Influence of silt content on shear strength of sandy soil", *IOP Conference Series: Earth and Environmental Science*, **768**(1), 12088.

Mohammadi, M., Fatemi Aghda, S.M., Talkhablou, M. andCheshomi, A. (2022), "Prediction of the shear strength parameters from easily-available soil properties by means of multivariate regression and artificial neural network methods", *Geomech. Geoeng.*, **17**(2), 442-454. https://doi.org/10.1080/17486025.2020.1778194.

Mollahasani, A., Alavi, A.H., Gandomi, A.H. and Rashed, A. (2011), "Nonlinear neural-based modeling of soil cohesion intercept", *KSCE J. Civil Eng.*, **15**, 831-840. https://doi.org/10.1007/s12205-011-1154-4.

Mousavi, S.M., Alavi, A.H., Gandomi, A.H. and Mollahasani, A. (2011), "Nonlinear genetic-based simulation of soil shear strength parameters", *J. Earth Syst. Sci.*, **120**, 1001-1022. https://doi.org/10.1007/s12040-011-0119-9.

Mujtaba, H. (2014), "Effect of void ratio and gradation on shear strength parameters of granular soils", *Pakistan J. Sci.*, **66**(3).

Murthy, V.N.S. (2002), *Geotechnical engineering: principles and practices of soil mechanics and foundation engineering*, CRC press.

Nguyen, B.Q.V. and Kim, Y.T. (2021), "Landslide spatial probability prediction: a comparative assessment of naive Bayes, ensemble learning, and deep learning approaches", *Bull. Eng. Geol. Environ.*, **80**, 4291-4321. https://doi.org/10.1007/s10064-021-02194-6.

Nguyen, B.Q.V., Song, C.H. and Kim, Y.T. (2022), "A hybrid physical and machine learning model for assessing landslide spatial probability caused by raising of ground water table and earthquake in Atsuma, Japan—case study", *KSCE J. Civil Eng.*, **26**(8), 3416-3429. https://doi.org/10.1007/s12205-022-1656-2.

Ojuri, O.O. (2013), "Predictive shear strength models for tropical lateritic soils", *J. Eng.*, 2013. https://doi.org/10.1155/2013/595626.

Palani, K.A., Maurya, S., Gupta, M. and Chitra, R. (2020), "Degree of initial saturation and shear strength of soil in a triaxial loading", *Int. J. Emerg. Technol. Innov. Res.*, **7**(4), 805-812.

Pereira, L., Godinho, L. and Branco, F.G. (2023), "Predicting unconfined compression strength and split tensile strength of soil-cement via artificial neural networks", *Geomech. Eng.*, **33**(6), 611-624. https://doi.org/10.12989/gae.2023.33.6.611.

Pham, B.T., Hoang, T.A., Nguyen, D.M. and Bui, D.T. (2018), "Prediction of shear strength of soft soil using machine learning methods", *Catena*, **166,** 181-191. https://doi.org/10.1016/j.catena.2018.04.004.

Probst, P., Wright, M.N. and Boulesteix, A. (2019), "Hyperparameters and tuning strategies for random forest", *Wiley Interdisciplinary Reviews: Data Mining and Knowledge Discovery*, **9**(3), e1301.

Quang, V.N.B., Viet, L.D., Chi, C.N., Duc, P.V.N. and Quang, B. N. (2021), "Predicting landslide spatial probability in Quang Ngai, Vietnam using deep learning technique", *Proceedings of the 4th Asia Pacific Meeting on Near Surface Geoscience & Engineering*, **2021**(1), 1-5.

Roman, M.J. (2014), *Correlation between shear strength at plastic limit and liquid limit Incorporating electrical resistivity*.

Roy, S. and Dass, G. (2014), "Statistical models for the prediction of shear strength parameters at Sirsa, India", *Int. J. Civil Struct. Eng.*, **4**(4), 483.

Roy, S., Prajapati, A.K. and Maurya, A.K. (2019), "Prediction of shear strength parameters using multiple regression analysis", *Int. J. Landscape Plann. Architect.*, **5**(2), 26-39.

Sahin, E.K. (2020), "Assessing the predictive capability of ensemble tree methods for landslide susceptibility mapping using XGBoost, gradient boosting machine, and random forest", *SN Appl. Sci.*, **2**(7), 1308. https://doi.org/10.1007/s42452-020-3060-1.

Salari, P., Lashkaripour, G. and Ghafoori, M. (2015). "Presentation of empirical equations for estimating internal friction angle of SP and SC soils in Mashhad, Iran using standard penetration and direct shear tests and comparison with previous equations", *Int. J. Geograph. Geol.*, **4**(5), 89. https://doi.org/10.4236/ojg.2015.55021.

Shahani, N. M., Kamran, M., Zheng, X., Liu, C. and Guo, X. (2021). "Application of gradient boosting machine learning algorithms to predict uniaxial compressive strength of soft sedimentary rocks at Thar Coalfield", *Adv. Civil Eng.*, **2021**, 1-19. https://doi.org/10.1155/2021/2565488.

Sharif Razavian, A., Azizpour, H., Sullivan, J. and Carlsson, S. (2014). CNN features off-the-shelf: an astounding baseline for recognition", *Proceedings of the IEEE Conference on Computer Vision and Pattern Recognition Workshops*.

Sharma, B. and Bora, P.K. (2003). "Plastic limit, liquid limit and undrained shear strength of soil—reappraisal", *J. Geotech. Geoenviron. Eng.*, **129**(8), 774-777. https://doi.org/10.1061/(ASCE)1090-0241(2003)129:8(774).

Shin, H.C., Roth, H.R., Gao, M., Lu, L., Xu, Z., Nogues, I., Yao, J., Mollura, D. and Summers, R.M. (2016), "Deep convolutional neural networks for computer-aided detection: CNN architectures, dataset characteristics and transfer learning", *IEEE T. Med. Imaging*, **35**(5), 1285-1298. https://doi.org/10.1109/TMI.2016.2528162.

Stefanow, D. and Dudziński, P.A. (2021). "Soil shear strength determination methods–State of the art", *Soil Tillage Res.*, **208**, 104881. https://doi.org/10.1016/j.still.2020.104881.

Thirugnanam, H. (2023), "Deep learning in landslide studies: A review", *Progress in Landslide Res. Tech.*, **1**(2), **2022**, 247-255.

Tripathi, M. (2021). "Analysis of convolutional neural network based image classification techniques", *J. Innov. Image Process.*, **3**(2), 100-117. 10.36548/jiip.2021.2.003.

Uncuoglu, E., Latifoglu, L. and Kaya, Z. (2023), "A hybrid approach to predict the bearing capacity of a square footing on a sand layer overlying clay", *Geomech. Eng.*, **34**(5), 561-575. https://doi.org/10.12989/gae.2023.34.5.561.

Wang, Y., Fang, Z. and Hong, H. (2019), "Comparison of convolutional neural networks for landslide susceptibility mapping in Yanshan County, China", *Sci. Total Environ.*, **666**, 975-993. https://doi.org/10.1016/j.scitotenv.2019.02.263.

Watabe, Y., Sassa, S., Kaneko, T. and Nakata, Y. (2017), "Mechanical characteristics of undisturbed coral gravel soils: The intergranular void ratio as a common governing parameter", *Soils Found.*, **57**(5), 760-775. https://doi.org/10.1016/j.sandf.2017.08.007.

Xia, Y., Liu, C., Li, Y. and Liu, N. (2017), "A boosted decision tree approach using Bayesian hyper-parameter optimization for credit scoring", *Exp. Syst. Appl.*, **78**, 225-241. https://doi.org/10.1016/j.eswa.2017.02.017.

Yoseph, H. (2022), *Estmation of soil shear strength parameters from index properties using ANN the case of ADDIS ABABA*.

Yoshida, Y., Kuwano, J. and Kuwano, R. (1991), "Effects of saturation on shear strength of soils", *Soils Found.*, **31**(1), 181-186. https://doi.org/10.3208/sandf1972.31.181.

Zakharov, A., Shenkman, R., Ofrikhter, I. and Ponomaryov, A. (2022), "Estimation of soil properties by an artificial neural network", *Mag. Civil Eng.*, **110**(2), 11011. https://doi.org/10.34910/MCE.110.11.

Zhang, W., Wu, C., Zhong, H., Li, Y. and Wang, L. (2021), "Prediction of undrained shear strength using extreme gradient boosting and random forest based on Bayesian optimization", *Geosci. Front.*, **12**(1), 469-477. https://doi.org/10.1016/j.gsf.2020.03.007.

Zhong, Y., Zhao, L., Liu, Z., Xu, Y. and Li, R. (2010), "Using a support vector machine method to predict the development indices of very high water cut oilfields", *Petroleum Sci.*, **7**, 379-384. https://doi.org/10.1007/s12182-010-0081-1.

Zhou, J., Li, E., Wei, H., Li, C., Qiao, Q. and Armaghani, D.J. (2019), "Random forests and cubist algorithms for predicting shear strengths of rockfill materials", *Appl. Sci.*, **9**(8), 1621. https://doi.org/10.3390/app9081621.

Zhu, L., Liao, Q., Wang, Z., Chen, J., Chen, Z., Bian, Q. and Zhang, Q. (2022), "Prediction of soil shear Strength parameters using combined data and different machine learning models", *Appl. Sci.*, **12**(10), 5100. https://doi.org/10.3390/app12105100.

IC